Separation and Purification Technology 189 (2017) 296–309

Contents lists available at ScienceDirect

Separation and Purification Technology

journal homepage: www.elsevier.com/locate/seppur

Screening of pervaporation membranes for the separation of methanol-methyl acetate mixtures: An approach based on the conceptual design of the pervaporation-distillation hybrid process

Danilo A. Figueroa Paredes[a], Daniela S. Laoretani[a], Juan Zelin[b], Rafael Vargas[a], Aldo R. Vecchietti[a], José Espinosa[a,c,*]

[a] Instituto de Desarrollo y Diseño INGAR (CONICET – UTN), Avellaneda 3657, 3000 Santa Fe, Argentina
[b] Instituto de Investigación en Catálisis y Petroquímica "ING. JOSE MIGUEL PARERA" INCAPE – CONICET, Colectora Ruta Nac. N° 168 km 0 – Paraje El Pozo, 3000 Santa Fe, Argentina
[c] Universidad Nacional del Litoral, Facultad de Ingeniería Química, Santiago del Estero 2829, 3000 Santa Fe, Argentina

ARTICLE INFO

Keywords:
Methanol-methyl acetate mixtures
Pervaporation
Membrane performance
Hybrid process
Conceptual modeling
Optimization

ABSTRACT

In this work, the pervaporation-distillation hybrid process is proposed to accomplish the separation of the azeotropic mixture methanol-methyl acetate.

First, the separation performance of four membranes of a medium-high flux (Pervap 2256, Pervap 2255-30, PolyAl TypM1 and PolyAn) is analyzed with the aid the pervaporation separation index (PSI). For the commercial Pervap 2256 membrane, pervaporation experiments were conducted to characterize its separation performance especially at compositions of the mixture around the azeotrope.

Then, a novel screening approach, which is based on the overall cost of the separation corresponding to the optimal Hybrid process design, is proposed. For feed compositions in the range 0.1–0.9 mol/mol, several process configurations are optimized varying the compositions of the retentate and distillate streams. Quasi-optimal operation temperatures, with correspond to maximum feasible ones, are 348.15 K for the Pervap membranes and 363.15 K for the PolyAn membranes, respectively. The studied membranes are successfully and consistently classified by their respective total cost. The designs corresponding to PolyAl TypM1 and Pervap 2256 membranes present the lowest overall costs.

Finally, detailed costs of the vacuum condensing system were also taken into account for the case of the Pervap 2256 membrane to include the permeate pressure as an optimization variable. The optimal value of the permeate pressure is 100 mbar and the corresponding condensation temperature is about 272 K.

1. Introduction

Pervaporation is a membrane process used to separate liquid mixtures. A feed mixture contacts one side of the membrane (the retentate side) while the permeate is removed as a vapor from the other side. The difference in chemical potential of components at both sides of the membrane is the driving force for the separation [1]. Separation success depends primarily on membrane type selection [2]. Potential applications of pervaporation are found in the separation of azeotropic binary mixtures and alcohols dehydration. Thermodynamic constraints impose high costs for traditional processes like conventional distillation or extractive distillation [3]. The advantage of the pervaporation process is its low energy consumption when compared with distillation because only partial vaporization of the feed is needed [4]. Moreover, thermodynamic constraints are overcome when using this technology for the separation of azeotropic mixtures. In some cases, however, reaching a desired separation specification using pervaporation requires high membrane areas making the standalone process economically unfeasible. As a consequence, in many cases the optimal solution is a hybrid process combining pervaporation with distillation [4–7]. Lipnizki et al. [8] showed a detailed list of pervaporation-based hybrid processes and their applications for several industrial purposes.

The methanol-methyl acetate mixture, which in turn presents an azeotrope, is a by-product of polyvinyl alcohol (PVA) production. There is a special interest in the separation of this mixture because whilst methanol is a feedstock in PVA production [9], methyl acetate can be converted into valuable products [9–12]. On industrial scale, advanced separation methods such as extractive distillation with water [3,13] or

* Corresponding author at: Instituto de Desarrollo y Diseño INGAR (CONICET – UTN), Avellaneda 3657, 3000 Santa Fe, Argentina.
E-mail address: destila@santafe-conicet.gov.ar (J. Espinosa).

http://dx.doi.org/10.1016/j.seppur.2017.08.027
Received 6 June 2017; Received in revised form 8 August 2017; Accepted 9 August 2017
Available online 10 August 2017
1383-5866/

Nomenclature

A,A_{min}	actual and minimal membrane area (m^2)
A_{Ci},A_{Bi}	condenser and reboiler heat exchanger areas of the C_i (m^2)
A_R	heat exchanger area needed for retentate reheating (m^2)
A_{VC},A_{RC}	vacuum and refrigerant condenser heat exchanger areas (m^2)
a, b, c	parameters used in Eq. (2)
B_i	bottom flow rate of the distillation column i (kmol/h)
C	parameter used in Eq. (3) (kmol/(m^2 h))
C_i	distillation column I
D_i	distillate flow rate the distillation column i (kmol/h)
Δt	time period (h)
E_a	apparent activation energy (kJ/mol)
F	flow rate of the pervaporation feed (kmol/h)
F_0	flow rate of the main feed stream (kmol/h)
F_i	flow rate of feed of the distillation column I (kmol/h)
J	total flux (kmol/ (h m^2))
J_i	molar flux of compound i (kmol/ (h m^2))
n_1, n_2	parameters used in Eq. (3)
n_P	collected permeate (kmol)
p	permeate pressure (bar)
P	permeate flow rate (kmol/h)
PSI	pervaporation separation index (kg/(h m^2))
Q_R	retentate heating duty (kW)
Q_P	permeate condensing duty (kW)
Q_{Ci},Q_{Bi}	condenser cooling and reboiler heating duties in C_i (kW)
R	retentate flow rate (kmol/h)
R	universal gas constant (kJ/(mol K))
T	temperature (K)
T_{op}	operating temperature in the pervaporation unit (K)
T_{cond}^{end}	condensation temperature at the end of the vacuum condenser (K)
W_{Comp}	power consumption of the refrigerant compressor (kW)
W_P,W_{VP}	power consumption of the recirculation and vacuum pumps (kW)
x_i, y_i	retentate and permeate composition of component i (mol/mol)
x_0	methanol composition in F_0 (mol/mol)
x_F	methanol composition in F (mol/mol)
x_{Bi}	methanol composition in B_i (mol/mol)
x_{Di}	methanol composition in D_i (mol/mol)
x_R	methanol composition in R (mol/mol)
y_P	methanol composition in P (mol/mol)

Subscripts

i	component: methanol, methyl acetate

Greek symbols

α	coefficient of separation or separation factor

pressure-swing distillation [14] are used to overcome the azeotrope.

Respect to pervaporation, there is not enough bibliography on the behavior of pervaporation membranes for the separation of the methanol-methyl acetate mixture. Initially, Sain et al. [15] analyzed a cuprophane membrane at 303.15 and 318.15 K. In their work, they also included the effect of permeate pressure on flux and selectivity. To this end, the permeate pressure was varied in the interval between 5 to 100 mbar. Steinigeweg and Gmehling [9] studied the commercial Pervap 2255-40, 2255-50 and 2255-60 membranes at 318.15 K and a permeate pressure of < 7 mbar. Gorri et al. [16] assessed the behavior of the Pervap 2255–30 membrane between 313.15 and 333.15 K for a permeate pressure < 4 mbar. In addition, they performed a comparative analysis with the up to that time reported membranes showing that Pervap 2255-30 membrane has the highest separation capability (PSI). Brinkmann et al. [17] showed a preliminary comparison between Pervap 2255-30 and 2256 membranes in terms of flux and selectivity at 323.15 K and permeate pressure of 10 mbar. The Pervap 2256 membrane showed a higher flux and lower selectivity than the 2255-30 one. A thoroughly study for the PolyAn membrane from 323.15 to 363.15 K and 1 mbar was dedicated in the technical report at Carl Von Ossietzky University [18]. Recently, Genduso et al. [3] performed a study for PolyAl TypM1 membrane between 303.15 and 317.15 K and a permeate pressure < 10 mbar. The PolyAl TypM1 membrane showed a high flux with a low/medium separation factor.

For the methanol-methyl acetate mixture, a temperature about 327.15 K corresponds to the maximum pressure azeotrope at 1.01 bar. For operating temperatures above this value, operating pressures above the atmospheric one should be applied in the retentate side in order to avoid a partial vaporization of the mixture. The maximum allowable working temperature depends on each membrane e.g. Pervap membranes can operate up to 353 K (SULZER Chemtech GmbH), PolyAn and PolyAl TypM1 up to 363.15 and 373.15 K, respectively [18,19]. Except for PolyAn membrane [18], all the mentioned studies [3,9,15,16] performed experiments at temperatures well below the maximum allowable temperatures. Given that the temperature is a very important variable for the pervaporation performance, designs at the reported temperatures would lead to high membrane area requirements. Therefore, to avoid economically unfeasible designs, it would be interesting to include the effect of the temperature on the membrane performance, especially at values near the maximum allowable.

Except for Sain et al. [15], all the mentioned studies showed experimental results at vacuum pressures below 10 mbar. As a consequence, condensing temperatures below 240 K are required to condense the permeate. Since both methanol and methyl acetate have freezing points below 180 K, there is not a tight constraint on the minimum permeate condensing temperature. In the design of the pervaporation unit, there is usually a trade-off between the operating cost of the vacuum condensing system and the investment cost of the membrane module. By considering the permeate pressure as an optimization variable, the mentioned trade-off is taken into account giving rise to optimal designs [20].

In order to achieve the separation of this mixture, all the mentioned authors recommended coupling the pervaporation unit to distillation columns into a hybrid process. Genduso et al. [3] proposed a retrofitting alternative to a conventional extractive distillation process. The retrofitting alternative considers two distillation columns and a pervaporation unit specially dedicated to break the azeotrope. Both alternatives were compared in terms of energy consumption. The obtained results demonstrate that the hybrid process assisted even with low separation factor membranes is a proper way to reduce the energy demand of the process.

The Pervaporation Separation Index (PSI) is not the best option to judge the performance of a pervaporation unit coupled to a distillation unit into a hybrid process [21]. Instead, a preliminary process cost estimation and optimization with the aid of shortcut or conceptual models is more appropriate to capture process trade-offs.

In the context of optimization-based design, Marquardt et al. [22] proposed a three-steps approach for the design of hybrid processes: (i) generation of flow-sheet alternatives, (ii) evaluation of the alternatives with the aid of shortcut methods; (iii) rigorous optimization of the most promising alternatives to obtain the best flow-sheet. In this line, Caballero et al. [23] successfully applied the last two steps of the mentioned approach in the optimization of a hybrid separation system composed by a distillation column and a vapor permeation unit.

Considering detailed rate-based models for distillation and pervaporation, Koch et al. [24] optimized a superstructure of the hybrid process using evolutionary algorithms for the simultaneous determination of the optimal process configuration, equipment design and operating conditions. In order to bridge the gap between shortcut calculations and a detailed engineering design, Skiborowski et al. [25] proposed an efficient and robust approach for the optimal design of membrane-assisted distillation processes. The mentioned authors also considered the operation of the pervaporation unit at high permeate pressures in order to reduce the operating cost required for the permeate condensation. Besides summarizing relevant contributions reached in this filed, Skiborowski et al. [25] validated the results obtained in previously reported shortcut-based designs like those presented by Bausa and Marquardt [4].

The aim of this manuscript consists on the preliminary choice of pervaporation membranes to be used in a hybrid distillation-pervaporation process. For this purpose, the methodology considered here intends to assess the performance of each pervaporation membrane resorting to estimations of the overall cost of separation of the hybrid process. When limited information for the membrane or distillation processes is available, an approach based on conceptual level design has a properly complexity to make a preliminary economic evaluation of the overall process while demanding only a reasonable effort in performing the task.

This task was performed resorting to conceptual models or shortcuts for each operation unit involved, which are characterized by their abilities to capture the essence of the process at low computational cost. The models adopted in this work consider the shortcut method presented by Bausa and Marquardt [4] for membrane area estimations and the McCabe-Thiele approach for the design of the distillation columns. Considering an additional cost model, this approach is suitable for the optimization-based design of several process configurations and pervaporation membranes. Thus, a proper comparison among the membranes can be made considering the economic figures corresponding to the optimal designs. In addition, a more detailed model of the vacuum condensing system is adopted to capture the process trade-off between the membrane module and the refrigeration system, which is scarcely considered in the design of pervaporation-distillation hybrid processes.

In this manuscript, the performance of the commercial Pervap 2256 membrane is analyzed for the separation of the methanol-methyl acetate mixture by pervaporation. Given that the performance of this membrane is scarcely reported in the literature, especially for the mentioned mixture, experiments at different temperatures and permeate pressures have been carried out in order to analyze their effect on flux and selectivity, especially for feed compositions around that of the azeotrope.

Subsequently, a performance comparison among Pervap 2256, Pervap 2255-30, PolyAl TypM1 and PolyAn membranes is performed. The separation performance is assessed resorting to the optimization of their respective pervaporation-distillation hybrid process. The design of each hybrid process is achieved with the aid of conceptual models of the operation units involved. In order to make a proper comparison of the separation performance, the overall separation cost for each membrane is taken at the optimal conditions of the corresponding hybrid process. For the case of the Pervap 2256 membrane, the conceptual model of the pervaporation unit considers the detailed design of the vacuum condensing system. Thus, the permeate pressure is included as an optimization variable.

2. Materials and methods

2.1. Pervaporation experiments

In this Section, the experimental procedure and the models used to describe the performance of the Pervap 2256 membrane are presented.

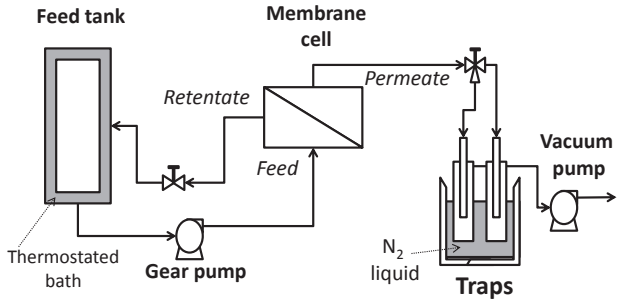

Fig. 1. CELFA Laboratory P-28 unit.

2.1.1. Materials

Analytical grade (99.8%) Methanol (MeOH, Cicarelli) and Methyl Acetate for synthesis (MeOAc, Merck) were used to prepare feed mixtures. A commercial PERVAP™ 2256 membrane supplied by SULZER Chemtech GmbH was operated at different temperatures. The maximum working temperature for this membrane is 353 K. Main applications of this membrane are the removal of methanol and ethanol from organic mixtures.

2.1.2. Equipment

For pervaporation experiments, a CELFA Laboratory P-28 unit provided with a feed tank of 0.5 L was used (Fig. 1). This equipment allows the use of membrane discs of 75 mm diameter with a membrane effective area of 28 cm^2. Recirculation flow rate is provided by a gear pump with flow velocities from 0.1 to 6 m/s. Retentate pressures from 0 to 8 bar can be set with a regulating valve. The feed tank temperature is kept constant with the aid of a thermostated bath. To allow continuous permeate sample collection, two traps in parallel, cooled with liquid nitrogen, are coupled to the permeate exit. A liquid ring vacuum pump is used to maintain the desired permeate pressure.

2.1.3. Experiments

Experiments were performed in a semi-batch setup. All experiments started with 0.45 L of a feed solution with 0.5 mol/mol of methanol. Before starting each experimental run, a new membrane was left overnight in contact with the feed solution at room temperature (~297 K). Four experiments were run, corresponding to three temperatures and two vacuum pressures as shown in Table 1. In all runs, the feed stream was fed to the membrane cell at a flow rate about 0.8 L/min. Due to the geometry of the membrane cell the corresponding Reynolds number is approximately between 9000 (318.15 K) and 12000 (348.15 K). These Reynolds values are sufficiently high to neglect both the temperature and concentration polarization effect on the permeate flux. Initially, permeate samples were collected each 15 min. After the first hour, the sampling time was progressively increased up to 60 min due to a decreasing behavior with time of the permeate flow rate. The retentate samples were collected each one permeate samples. The collected samples were weighed and stored for subsequent analysis by gas chromatography. The first samples of each run were not taken into account for the results.

In the performance characterization for the Pervap 2256 membrane carried out in this work, neither replicates nor long term experiments were considered. The adopted experimental approach is appropriate for the preliminary choice of pervaporation membranes from semi-

Table 1
Conditions of pervaporation experiment.

Temperature (K ± 1)	Feed pressure (bar ± 0.2)	Vacuum (mbar ± 1.5)
318.15	1.5	5
333.15	2.0	5, 100
348.15	2.5	5

empirical models (see Section 2.1.5) of the membrane behavior in a wide compositions range. A more detailed experimental task should only be applied for the final design step of the hybrid process. In order to validate our experimental results, flux and selectivity data obtained in our laboratory were compared with results obtained by Brinkmann et al. [17] under slightly different operating conditions. To make a proper comparison, flux and selectivity values were simulated running the semi-empirical model described in Section 2.1.5 under the conditions reported in Brinkmann et al. [17]. As can be seen in Figs. SM1 and SM2 (Supplementary material), a good agreement between our simulated data and the experimental points were achieved.

The permeate flux J_i of each component is calculated through Eq. (1).

$$J_i = \left(\frac{n_P}{A*\Delta t}\right)*y_i \tag{1}$$

where n_P is the permeate weight, Δt is the sample collection time, A is the effective membrane area, and y_i is the composition of component i in the permeate.

2.1.4. Analytical technique

The analysis of permeate and retentate samples were performed at the laboratory of INCAPE - CONICET. Quantitative analysis was done by the external standard method using propanol (3.6% w/v) in butanol as standard solutions. Methanol and methyl acetate concentrations were followed by ex-situ gas chromatography using an SRI chromatograph, equipped with flame ionization detector (FID) and a 30 m HP Innowax capillary column with a 0.25 mm coating.

2.1.5. Modeling

In principle, the objective of this work is the screening of different pervaporation membranes based on the conceptual design of the pervaporation-distillation hybrid process. To this end, either empirical or semi-empirical expressions are usually adopted to represent the pervaporation performance with an acceptable accuracy.

To describe the behavior of the permeate composition as function of the retentate composition, an empirical model for binary mixtures (Eq. (2)) is adopted. This expression, which has an adequate complexity, is used by Steinigeweg and Gmehling [9] in their work.

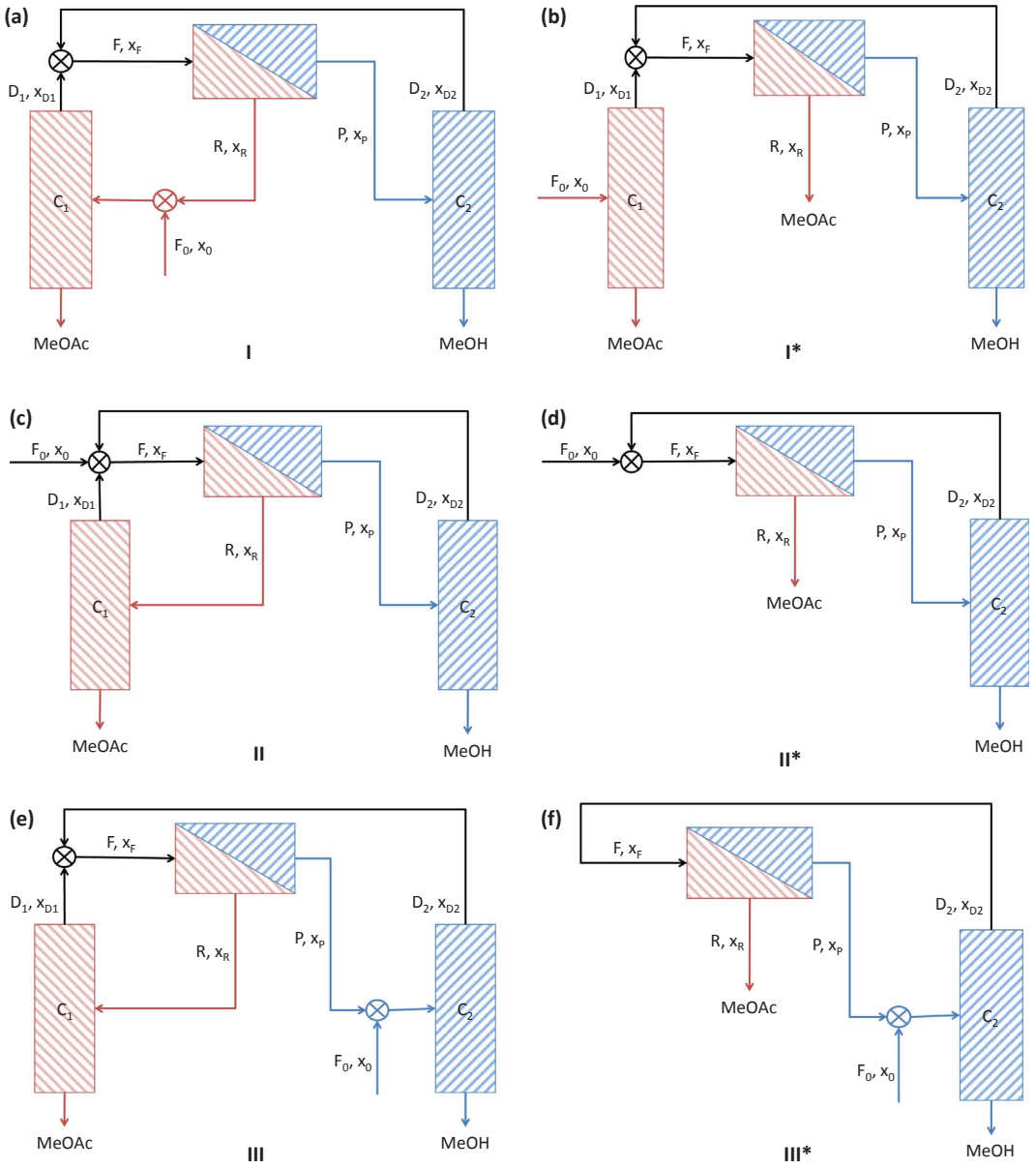

Fig. 2. Hybrid process configurations depending on the location of the main feed stream (a) I, (b) I*, (c) II, (d) II*, (e) III and (f) III*.

$$y_{MeOH}=x_{MeOH}/(a + b*x_{MeOH} + c*x_{MeOH}^2) \quad (2)$$

In Eq. (2), methanol composition in retentate and permeate sides are represented by x_{MeOH} and y_{MeOH}, respectively.

Gorri et al. [16] used a semiempirical expression with an Arrhenius-type equation to model the temperature dependence of the permeate flux. Koch and Górak [26] resorted to a power law expression to represent the feed composition effect on permeance. In this paper, the effects of retentate composition, temperature and vacuum pressure on permeate flux are taken into account through the following semi-empirical expression:

$$J_{MeOH} = C*x_{MeOH}^{n1}*p^{n2}*\exp\left(-\frac{E_a}{RT}\right) \quad (3)$$

In Eq. (3), the permeate pressure p and methanol composition in the retentate x_{MeOH} are raised to exponents n1 and n2, respectively. In the exponential part of Eq. (3), T is the temperature, R is the universal gas constant and E_a is the apparent activation energy. E_a, C factor, and exponents $n1$ and $n2$ are parameters of the model and their values are found through the least square method implemented in MATLAB environment [27]. The 95% confidence intervals corresponding to each model parameter in Eqs. (2) and (3) are estimated by performing a bootstrapping method [28,29].

The Pervaporation Separation Index (PSI) is then calculated using the Eq. (4) as suggested by Genduso et al. [30].

$$PSI = J*(\alpha-1) \quad (4)$$

where the separation factor α is calculated from the ratio $(y_{MeOH}/y_{MeOAc})/(x_{MeOH}/x_{MeOAc})$.

2.2. Membrane screening methodology

In this Section, the methodology used for the assessment of the separation performance for the different membranes considered in this paper is outlined.

2.2.1. Description of the different feasible hybrid process configurations

At atmospheric pressure, the mixture methanol-methyl acetate shows a low boiling azeotrope with a methanol composition about 0.336 mol/mol. To accomplish the separation of this mixture using distillation, complex systems like pressure swing distillation or extractive distillation are required. On the other hand, there are several pervaporation membranes with the capability to break this azeotrope. However, pervaporation is not suitable as a standalone process due to economical reasons. Therefore, the analysis of distillation and pervaporation coupled into a hybrid process is of interest when the complete separation of this mixture is desired. With the aim of reaching the most economical design of this hybrid process corresponding to each pervaporation membrane, several process configurations must be taken into account depending on the composition of the mixture to be separated.

The pervaporation-distillation hybrid process considered in this work is composed by up to two distillation columns and a pervaporation unit. Basically, the main feed stream with flow rate F_0 and composition x_0 is separated into two product streams, one of them rich in methanol and the other rich in methyl acetate. In Fig. 2, several configurations of the hybrid process are schematically illustrated. For the sake of brevity, only configuration II (Fig.2c) is described. In this configuration, the distillate streams D_1 and D_2 with compositions at both sides of the azeotrope; x_{D1} and x_{D2}, respectively, are mixed with the main feed stream resulting into a stream F, of composition x_F, which is fed to the pervaporation unit. From the pervaporation unit a methyl acetate-rich retentate stream R with composition x_R and a methanol-rich permeate stream P with composition x_P are obtained. The retentate stream is fed to distillation column C_1 in order to obtain an almost pure methyl acetate bottom stream (B_1,x_{B1}). On the other hand, the permeate stream is sent to column C_2 to obtain an almost pure methanol bottom product (B_2,x_{B2}).

Depending on the composition of the main feed stream, the hybrid process could be arranged in several configurations, being its location the main difference among them. Configuration I (Fig.2a) is feasible for methanol compositions lower than that of the azeotrope while configuration III (Fig.2e) is suitable for methanol compositions higher than that the azeotropic one. It is noteworthy that configuration II (Fig. 2c) is feasible for the entire composition interval. Besides main configurations I, II and III, possible variants I∗, II∗ and III∗, which are characterized by an almost pure methyl acetate retentate must be also taken into account.

The process design at the conceptual model level allows the achievement of an adequate process description while demanding only a reasonable effort in performing the task. The methodology considered here intends to assess the performance of each pervaporation membrane resorting to estimations of the overall cost of separation of the hybrid process.

In order to estimate overall costs, sizes and energy requirements for distillation and pervaporation units are calculated with the aid of conceptual models. The economic assessment takes into account both the investment and operating cost of each unit operation involved. For the sake of simplicity, the following assumptions are made: (i) only one stream is fed to each distillation column, (ii) reheating of the condensed permeate up to its bubble point is not considered in the calculation of the energy requirements of the pervaporation unit.

A degree of freedom analysis shows that after specification of the flow rate and composition of the main feed together with the compositions of the bottom streams of both distillation columns three freedom degrees remain. We selected the compositions of the retentate and the distillate streams as degrees of freedom. These variables are also taken as optimization variables to seek for the most economical design.

2.2.2. Conceptual model for distillation

Respect to thermodynamics properties, the vapor-liquid equilibrium non idealities are taken into account using the UNIQUAC equation. Ideal gas phase behavior is assumed. The binary interaction parameters and relative Vander Waals properties for the components of the mixture are taken from Pöpken et al. [31] while parameters for pure component properties calculated with DIPPR equations were taken from the Aspen Hysys database [32]. Thermodynamics properties are calculated considering that the distillation columns operate at atmospheric pressure. For the sake of simplicity, pressure drops corresponding to each column are neglected.

As it will be shown later, at each step of the optimization procedure, overall mass balances for both distillation columns will be at hand. Thus, minimum reflux estimations for given values of both distillate and bottom compositions can be done resorting to pinch theory [33]. The actual reflux ratio is then calculated by multiplying the minimal one by a factor of 1.2. With this value, reboiler and condenser energy requirements can be calculated together with the size of their respective heat exchangers. In this paper, the number of theoretical equilibrium stages and the locations of the feed stream are calculated through the McCabe-Thiele approach [34]. The number of actual trays is estimated assuming a tray efficiency of 65%, while the column diameter is calculated from the values of both actual vapor flow rate and flooding velocity [35].

2.2.3. Conceptual model for pervaporation

For modeling pervaporation processes, Bausa and Marquardt [4] proposed a shortcut method which is able to use complex mass-transfer models to describe the separation behavior through the pervaporation membrane. Assuming a one-dimensional module, an ordinary system of differential equations must be integrated in order to estimate both the membrane area requirement and the mass and energy balances around the unit.

Minimum membrane area requirement can be obtained by assuming a constant operating temperature along the pervaporation module. Actual membrane area is then calculated by multiplying the minimal one by a factor of 1.25. This model requires an infinite number of heat exchangers to maintain the operation temperature at a value corresponding to that of the feed stream [4].

As mentioned above, the composition of the retentate stream x_R is selected as an optimization variable. In this case, given the flow rate and the composition of the feed stream, the minimum membrane area requirement A_{min} is calculated in order to achieve the desired composition in the retentate stream. The permeate flow rate P, the retentate flow rate R and the heating duty of the retentate stream Q_R are also obtained by solving the model.

Fahmy et al. [20] proposed an integral form of the model equations presented in Bausa and Marquardt [4], which are valid for binary mixtures. Assuming a value for the composition of the retentate stream, the overall mass balance on the membrane module is solved for the retentate flow rate with the aid of Eq. (5). Note that in this case, the mass balance around the unit is solved without the need to iterate in the minimum membrane area as it is required when following the approach proposed in Bausa and Marquardt [4]. Once the overall mass balance is calculated, the minimum area requirement is estimated by solving Eq. (6). Then, the energy required to vaporize the permeate stream is computed resorting to Eq. (7).

$$R = F*exp\left(-\int_{x_R}^{x_F}\frac{dx'}{y'-x'}\right) \tag{5}$$

$$A_{min} = F*\int_{x_R}^{x_F} exp\left(-\int_{x'}^{x_F}\frac{dx''}{y''-x''}\right)\frac{1}{J(y'-x')}dx' \tag{6}$$

$$Q_R = -P*h^{vap} \tag{7}$$

In Eq. (5), the permeate local composition y is function of the retentate local composition x. In Eq. (6), the permeate local flux J depends on the retentante local composition and temperature, and on the permeate pressure. h^{vap} in Eq. (7) represents the vaporization enthalpy of the mixture, which depends on the permeate composition and temperature.

2.2.4. Conceptual model for the vacuum condensing system

The modeling of the vacuum condensing system is usually neglected at the design stage of the pervaporation-distillation hybrid process. Instead, some assumptions are made: (i) the energy requirement for permeate condensation is the same to that for retentate heating, (ii) the power consumption of both recirculation and vacuum pumps are neglected. Investment cost of the pervaporation unit including the vacuum condensing system is estimated assuming a value per membrane area (U$S/m^2). (iii) the refrigeration cost is estimated resorting to utility correlations.

The main advantage of considering a more detailed design of the vacuum condensing system is the achievement of more precise cost estimations. In addition, the trade-off between the investment cost of the membrane module and the operating cost of the vacuum system is captured by varying the value of permeate pressure into an optimization procedure.

The vacuum condensing system considered in this work is formed by a condenser and a vacuum pump. The vacuum condenser is coupled into a vapor compression refrigeration cycle using propane as refrigerant. A detailed description of this system can be found elsewhere [21]. To achieve an appropriate description of the phase change of the mixture along the condenser, a multi-node model is adopted. An inward leakage of air into the equipment under vacuum is unavoidable. Thus, an iterative procedure is required to simultaneously solve the mass and energy balances together with the sizing equations of the vacuum condenser [20]. Taking into account the air effect on the phase equilibrium, the condensation temperature at the end of the vacuum condenser T_{cond}^{end} is calculated assuming a 99.8% recovery of the condensable components. The non-condensate permeate is neglected in the overall mass balance. If the condensation temperature is very low, a multistep refrigeration cycle with two compressors is adopted. For the design of the refrigeration system, the temperature of the refrigerant in the vacuum condenser is assumed 15 K below the permeate condensation temperature (T_{cond}^{end}). On the other hand, in the refrigerant condenser a difference of 10 K is considered between the temperature of the refrigerant and the temperature of the cooling water. The energy consumptions corresponding to the compressor, the vacuum pump, and the recirculation pump are obtained by solving the model. It is noteworthy that in this case, the mass balance of the hybrid process cannot be decoupled from the sizing equations of the membrane unit and the vacuum condenser, making an iterative procedure unavoidable.

2.2.5. Solving and optimization procedures

Due to the presence of recycle streams in the hybrid process, the overall mass balance must be solved in an iterative way. As mentioned above, for most of the configurations shown in Fig. 2, three degrees of freedom remain in the design of the hybrid process. Two degrees of freedom must be considered, however for configurations having only one distillation column. As mentioned in Section 2.2.1, compositions of both retentate and distillate streams are selected both as degree of freedom and optimization variables.

Given values for x_R, x_{D1} and x_{D2}, the overall mass balance must be solved. To do that, flow rate and composition of the feed stream into pervaporation unit are taken as tear variables. Except for the vacuum condensing system, the conceptual models adopted in this manuscript allow decoupling mass balance calculations from equipments sizing and process energy demand estimations. Once the overall mass balance is converged, the equipments sizes and the energetic requirements are then calculated. With this information, economic figures can be estimated.

The investment costs of each operation unit are calculated using the correlations given in Supplementary material. For the membrane unit, the investment cost is estimated using overall cost factors per unit of membrane area. Although, if a detailed design of the vacuum condensing system is considered, the investment cost is calculated taken into account the purchase cost of the different equipments involved. Regarding to the operating costs of each unit, the corresponding energy requirements are converted into their respective utilities consumption like cooling water, steam, or electricity consumption. The membrane replacement in the pervaporation unit is also taken into account. If the design of the vacuum condensing system is considered, the operating cost related to permeate condensation is disaggregated into its respective utilities consumptions. Further explanations, regarding cost estimation can be found in Supplementary material.

Considering the minimization of the overall cost of separation, the optimization of the hybrid process design for each membrane is achieved varying the value of the composition of the retentate and distillate streams. For the optimization problem, the retentate composition is limited by the composition of the feed to pervaporation x_F and the bottom composition in distillation column C_1, while the distillate compositions x_{D1} and x_{D2} are constrained by the azeotrope composition and their respective feed composition. If the detailed design of the vacuum condensing system is considered, the permeate pressure is also included as an optimization variable.

All models were implemented in a MATLAB environment [27]. The solver NOMAD [36] employing the OPTI Toolbox [37] was used to carry out the optimization. Note that the solver NOMAD is specially designed to solve non-differentiable and global nonlinear programs (black box optimization).

2.2.6. Problem statement

The performance of four methanol selective membranes (Pervap 2255-30, Pervap 2256, Polyan and PolyAl TypM1) for the separation of

the methanol-methyl acetate mixture is analyzed. The information about flux and selectivity for the membranes Pervap 2255-30, Polyan and PolyAl TypM1 is taken from Gorri et al. [16], a technical report at Carl Von Ossietzky University [18] and Genduso et al. [3], respectively.

A first analysis is performed by comparing the PSI values corresponding to each membrane for retentate compositions in the interval between 0.2 and 0.5 mol/mol, which includes the azeotrope. This comparison is also performed at different values of temperature, especially at values near the maximum allowable, in the range between 318.15 and 363.15 K.

Given that the PSI fails in capturing essential trade-offs present in pervaporation-distillation hybrid processes, preliminary cost estimation is proposed instead to make a proper comparison of the separation performance of each membrane. A feed flow rate of 500 kmol/h is assumed to take into account chemical companies of medium-large scale. For all considered cases, the methanol-methyl acetate mixture is separated into two different product streams with methanol compositions of 0.056 and 0.99 mol/mol, respectively. These values were selected to allow a proper comparison with results obtained by Genduso et al. [3]. In order to establish the most economical hybrid process configuration, overall costs of separation are calculated for values of methanol composition of the main feed stream in the interval 0.1–0.9 mol/mol. Calculations are also performed for values of the operating temperature of the pervaporation unit between 318.15 and 363.15 K.

Due to the scarce cost data reported for membrane units [4], it is assumed that the purchase cost per membrane area of the membrane module is the same for all membranes considered in this paper. With the aim of considering possible variations in the investment cost among the membranes, a sensitivity analysis is performed by varying either the cost factors related to the purchase cost of the membrane module or the investment cost of the overall pervaporation unit.

Finally, a detailed design of the vacuum condensing system is performed for the Pervap 2256 membrane including the permeate pressure as an optimization variable (10–100 mbar).

3. Results and discussion

3.1. Performance of the Pervap 2256 membrane

For the Pervap 2256 membrane, permeate composition versus retentate composition self-obtained data are used to fit the model parameters in Eq. (2), which are shown in Table 2. Additionally, this table also reports the adjusted parameters for the PolyAn and PolyAl TypM1 membranes. For the last membranes, the model parameters are fitted using the data provided in the technical report at Carl Von Ossietzky University [18] and Genduso et al. [3], respectively.

For the Pervap 2256 membrane, Fig. 3a shows both experimental and calculated values for the permeate composition as function of the retentate composition. In the analyzed interval, the methanol composition in permeate is always higher than that in retentate, exhibiting the selective characteristic of this membrane for methanol. Fig. 3 also includes the vapor-liquid equilibrium (VLE) of the methanol-methyl acetate mixture at 1 atm. Comparing the permeate composition profile with the VLE line, it is concluded that this membrane is capable of splitting the methanol-methyl acetate azeotrope.

The experimental results displayed in Fig. 3 were obtained at different values of temperature and permeate pressure. Due to instruments inaccuracy, the maximum relative error in the compositions measurement is about ± 2% while for the total permeate flux, estimated with Eq. (1), the corresponding maximum relative error is about ± 5%. Assuming that the effect of temperature and permeate pressure on the permeate composition is negligible, the parameters in Eq. (2) are adjusted using all available data. The acceptable value obtained for the determinant coefficient R^2 of 0.9415 verifies the accordance with the mentioned assumption (Table 2). Similarly, the adjusted parameters for the PolyAn and PolyAl TypM1 membranes also are fitted neglecting the temperature effect on the permeate composition profile. For these membranes, high values for the determinant coefficients are obtained ($R^2 > 0.98$, Table 2). For the Pervap 2256 and PolyAl TypM1 membranes, the low value of the coefficient c (Table 2) point out that the use a second order term in the denominator in Eq. (2) is not relevant to model the permeate composition.

The experimental data for methanol flux against retentate composition are correlated with Eq. (3). Calculated parameters are shown in Table 3 for Pervap 2256, PolyAl TypM1 and PolyAn membranes, respectively. For all cases, the determinant coefficient R^2 is above 0.98.

For the Pervap 2256 membrane, Fig. 4a shows both experimental and calculated data for methanol molar flux at 318.15, 333.15 and 348.15 K and 5 mbar. From this figure, it is noteworthy that the methanol flux profile corresponding to 348.15 K is above those obtained at lower operation temperatures. In Fig. 4b, methanol flux profiles for two different permeate pressures (5 and 100 mbar) are displayed at 333.15 K. By analyzing Fig. 4b, it is concluded the permeate pressure has an opposite effect to that of temperature on the permeate flux, i.e. the highest fluxes are reached at the lowest value of the vacuum pressure.

For purposes of this work, models given by Eqs. (2) and (3) describe properly experimental and literature data. Note however that the permeate flux model should be carefully applied for permeate pressures out of the analyzed interval because the empirical model does not include a driving force type factor for the pressure.

3.2. PSI comparison

Models of flux and selectivity with parameters given in Tables 2 and 3 are used in the calculations needed to estimate the PSI values for the separation of the mixture using the Pervap 2256, PolyAl TypM1 and PolyAn membranes. For the Pervap 2255-30 membrane, the models and parameters given by Gorri et al. [16] are used instead.

Fig. 5 shows the separation factor as function of the retentate composition in the interval [0.2, 0.5 mol/mol]. The Pervap 2255-30 membrane presents the highest values of the separation factor while the PolyAl TypM1 membrane shows the lowest values. The separation factor corresponding to two remaining membranes are similar between them and their values are nearer to those corresponding to PolyAl TypM1 membrane. For all membranes, the separation factor presents a decreasing behavior with the methanol composition in the retentate. Calculations are performed neglecting the temperature effect on the separation factor. This assumption is in accordance with the observations made by Gorri et al. [16], Genduso et al. [3] and the technical report at Carl Von Ossietzky University [18].

In Fig. 6a, calculated overall flux versus retentate composition is shown for each studied membranes at 318.15 K. It can be seen that for all membranes the overall flux is proportional to the methanol composition in the retentate. For the Pervap 2256 and PolyAl TypM1 membranes, total fluxes are much higher than those for the PolyAn and Pervap 2255-30 membranes. Note that the results obtained for the

Table 2
Adjusted parameters to model the permeate composition as function of the retentate composition (Eq. (2)) and 95% confidence intervals.

Membrane	a	b	c	R^2
Pervap 2256	0.1392 (0.1000 0.1780)	1.317 (1.066 1.590)	−0.1809 (−0.6186 0.2195)	0.9415
PolyAl TypM1	0.1700 (0.1495 0.1952)	1.396 (1.193 1.539)	−0.3848 (−0.5648–0.0609)	0.9895
PolyAn	0.1011 (0.0856 0.1115)	1.624 (1.565 1.694)	−0.7289 (−0.7929–0.6732)	0.9965

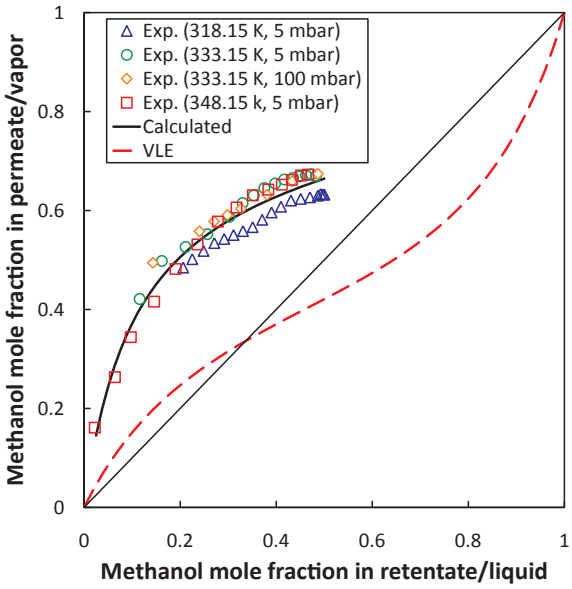

Fig. 3. Permeate composition as function of retentate composition for the PERVAP 2256 membrane.

Table 3
Adjusted parameters to model the methanol permeate flux (Eq. (3)) and 95% confidence intervals.

Membrane	C (kmol/(m^2 h))	E_a (kJ/mol)	$n1$	$n2$	R^2
Pervap 2256	1.496e03	23.90	1.1709	−0.1461	0.9966
	(1.098e03	(23.09	(1.1245	(−0.1586–0.1238)	
	2.085e03)	24.65)	1.2130)		
PolyAl TypM1	0.9648e05	33.10	1.363	–	0.9832
	(0.0678e05	(26.27	(1.229		
	9.4300e05)	38.96)	1.508)		
PolyAn	307.0	20.64	0.9951	–	0.9912
	(138.3	(18.42	(0.9168		
	539.9)	22.29)	1.0557)		

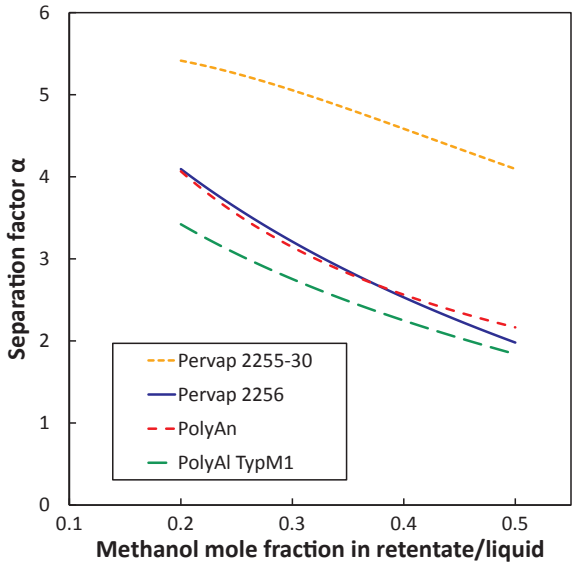

Fig. 5. Separation factor versus retentate mole fraction.

PolyAn membrane were extrapolated for methanol compositions lower than 0.2 mol/mol using the model described in the Section 2.1.5 (Eqs. (2) and (3)).

To take into account the temperature effect on the overall flux, calculations were also performed at 348.15 K as can be seen in Fig. 6b. In all cases an increasing behavior of overall flux with temperature is found. The overall flux increases approximately three times for the PolyAl TypM1 membrane and only twice for the other membranes when the temperature is increased only 30 K. It is important to highlight that the calculations performed for the PolyAl TypM1 membrane at 348.15 K were extrapolated from data between 303.15 and 317.15 K [3] using the model exposed in the Section 2.1.5. Further experiments are required to corroborate the behavior shown in Fig. 6b. For the Pervap 2255-30 membrane, the calculations were performed using the model presented by Gorri et al. [16] with experiments performed at temperatures below 333.15 K.

Fig. 7a and b show the calculated PSI values at 318.15 and 348.15 K, respectively. For the membranes Pervap 2256, PolyAl TypM1

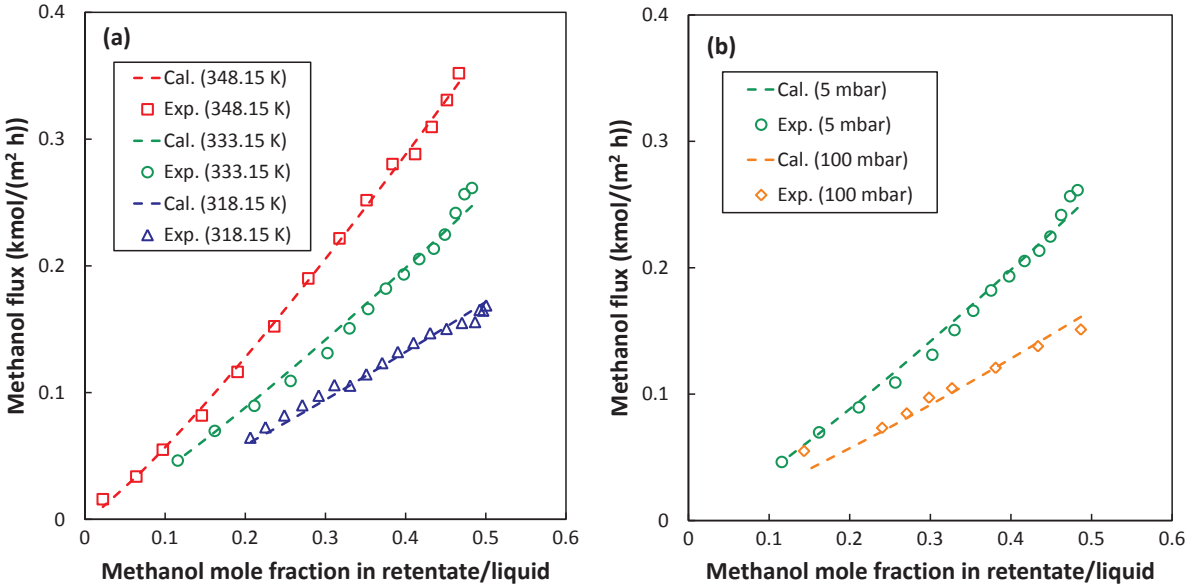

Fig. 4. Effect of (a) temperature (318.15, 333.15 and 348.15 K; 5 mbar) and (b) permeate pressure (5 and 100 mbar; 333.15 K) on the permeate flux of methanol for the PERVAP 2256 membrane.

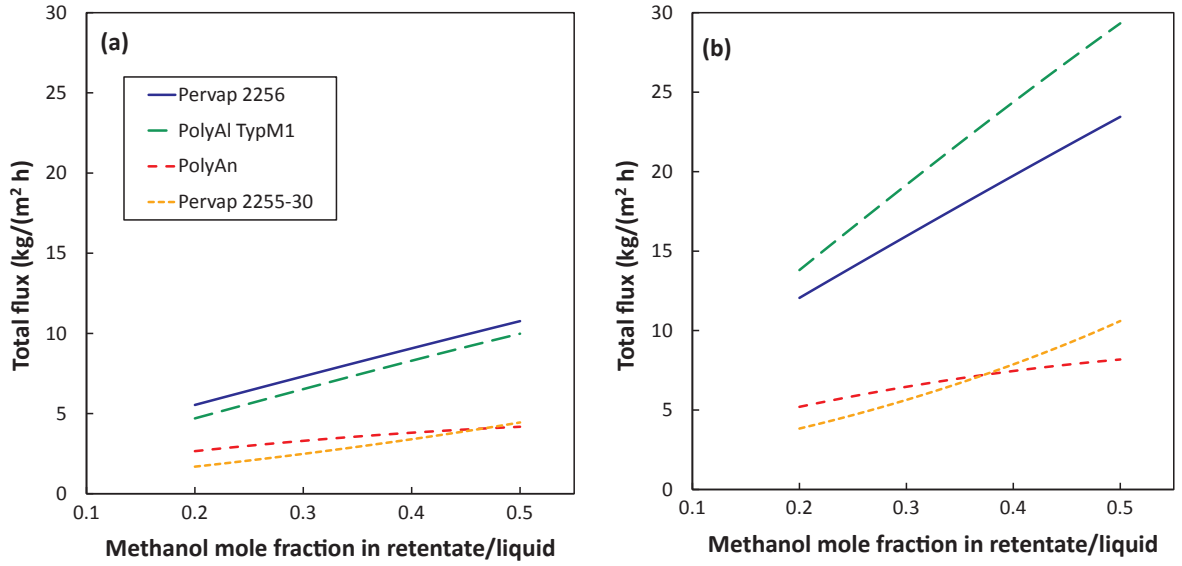

Fig. 6. Total flux vs. retentate composition at (a) 318.15 and (b) 348.15 K.

and PolyAn at 318.15 K, the PSI presents a decreasing behavior with the methanol mole fraction in the retentate. Among these membranes, the Pervap 2256 membrane shows the highest PSI values while the PolyAn membrane presents the lowest ones. For the Pervap 2255-30 membrane, the calculated PSI presents an increasing behavior with the methanol composition. The performance of this membrane surpasses that of the others for methanol mole fractions above 0.45.

From the comparison between Fig. 7a and b it is noted that the PSI values increase proportionally with temperature for all membranes. Particularly, the increment for the PolyAl TypM1 membrane is much higher than that of the others.

As mentioned above, Pervap membranes can operate at temperatures up to 358.15 K while experimental data at operating temperatures as high as 363.15 and 373.15 K were obtained for PolyAn and PolyAl TypM1 membranes, respectively.

Due to the high PSI values expected at higher temperatures, it is advisable to operate the pervaporation unit near the maximum working temperature in order to achieve designs with the lowest feasible membrane area requirements. In accordance with this, PSI values in Fig. 8 are calculated at 363.15 K for the PolyAn and PolyAl TypM1 membranes and at 348.15 K for the Pervap membranes. Note that PSI values corresponding to the PolyAl TypM1 membrane are well above than those corresponding to the other membranes.

3.3. Hybrid process design

As mentioned in Section 2.2.6, the PSI fails in capturing essential trade-offs present in pervaporation-distillation hybrid processes. Therefore, preliminary cost estimations are performed in this section. To make a proper comparison of the separation performance of each membrane different process configurations are taken into account.

For all considered cases in this manuscript, a main feed stream with a flow rate of 500 kmol/h is separated into two different product streams with methanol compositions of 0.056 and 0.99 mol/mol, respectively.

Let us analyze, for the sake of comprehension, the separation of a methanol-methyl acetate mixture of composition 0.5 mol/mol. In this case, an operating temperature of 348.15 K is adopted for the pervaporation unit. For all membranes, Table 4 presents the mass balances corresponding to the optimal design of the hybrid process configuration

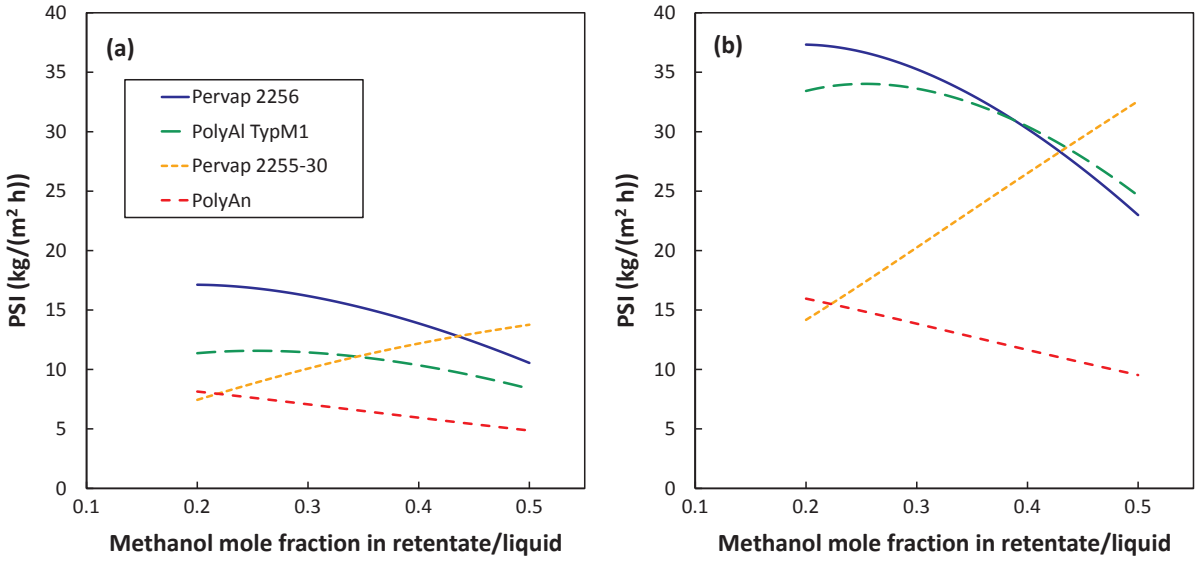

Fig. 7. Pervaporation Separation Index (PSI) versus retentate composition at (a) 318.15 and (b) 348.15 K.

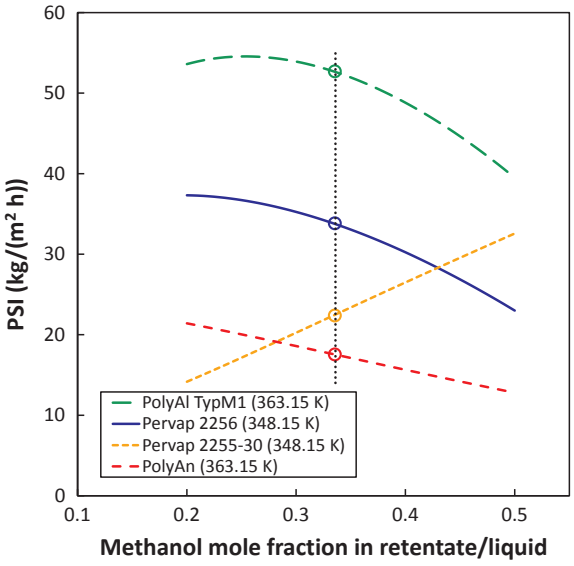

Fig. 8. Pervaporation Separation Index (PSI) versus retentate composition. The dotted vertical line highlights results at the azeotropic composition.

Table 4
Mass balance of the hybrid process configuration III for different commercial membranes (F_0 = 500 kmol/h, x_0 = 0.5 mol/mol, T_{op} = 348.15 K).

	Membranes			
	PolyAl TypM1	PolyAn	Pervap 2255-30	Pervap 2256
F (kmol/h)	927	858	876	811
x_F (mol/mol)	0.343	0.338	0.337	0.346
R (kmol/h)	468	494	609	415
x_R (mol/mol)	**0.173**	**0.181**	**0.207**	**0.152**
P (kmol/h)	458	364	268	396
y_P (mol/mol)	0.517	0.553	0.634	0.550
F_1 (kmol/h)	468	494	609	415
x_{F1} *(mol/mol)*	0.173	0.181	0.207	0.152
D_1 (kmol/h)	206	232	346	153
x_{D1}(mol/mol)	**0.322**	**0.322**	**0.321**	**0.316**
F_2 (kmol/h)	958	864	768	896
x_{F2}(mol/mol)	0.508	0.522	0.547	0.522
D_2 (kmol/h)	721	626	530	658
x_{D2} (mol/mol)	**0.350**	**0.345**	**0.348**	**0.353**

III. In this table, values for optimization variables are shown in bold.

Among the membranes, the optimal value of the retentate composition x_R varies between 0.152 and 0.207 mol/mol. For the distillate compositions x_{D1} and x_{D2}, the optimal values are in the intervals [0.316, 0.322] and [0.348, 0.353 mol/mol], respectively. From the comparison of the optimal values for the mentioned variables, it emerges that the optimal solution of the retentate composition is very different for each membrane.

In Table 5, equipments sizes and their corresponding energy duties at the optimum are shown. The last row of Table 5 also shows the overall cost of separation which comprises both the investment and operating costs.

The design corresponding to the PolyAn membrane presents the highest membrane area requirement, about 3850 m^2, while the designs corresponding to the Pervap 2256 and PolyAl TypM1 membranes shows the lowest membrane area requirements being these about the half than that for the PolyAn one. Although the area requirements for the PolyAl TypM1 and Pervap 2256 membranes are very similar between them, the retentate heating duties demanded for these membranes are very different. The retentate heating duty for the Pervap 2256 membrane is 13% lower than that corresponding to the PolyAl TypM1 one, while the design with the lowest retentate heating duty corresponds to the Pervap 2255-30 membrane.

Regarding to the distillation task, the optimal design corresponding to the Pervap 2256 membrane presents the lowest number of trays in both distillation columns given that their respective distillate compositions are the most distant from the azeotrope. Moreover, the design corresponding to this membrane shows the lowest overall energy demand. On the other hand, the design with the PolyAl TypM1 membrane presents the highest overall energy demand, which is 15% above the corresponding to the design with the Pervap 2256 membrane.

From the economic figures (last row in Table 5), the overall costs for the designs corresponding to the PolyAl TypM1, Pervap 2255-30, and PolyAn membranes are 11, 25 and 41% above the corresponding to the Pervap 2256 membrane, respectively. Although the investment cost of the membrane area for the PolyAl TypM1 membrane is lower than that the corresponding to the Pervap 2256 one, the higher operating costs involved in the design with the PolyAn TypM1 membrane make this alternative unfavorable, being it relegated to the second place after the alternative with the Pervap 2256 membrane.

Broadening the analysis above to feed compositions between 0.1 and 0.9 mol/mol, both technical and economic feasibility issues are now considered for all proposed process configurations. Fig. 9a and b show the overall cost of separation as function of the main feed composition for the designs corresponding to the Pervap 2255-30 and 2256 membranes, respectively. Each point in Fig. 9a and b corresponds to the optimal design of the respective hybrid process configuration. For all membranes, detailed results corresponding to the optimal process configurations are presented in Tables SM1–SM18 (Supplementary material). From Fig. 9a and b, it is noted that for both membranes the overall cost of separation is lower when the composition of the main

Table 5
Equipments sizes, energy requirements and overall cost of the hybrid process configuration III for different membranes. Values reported correspond to the optimal mass balances in Table 4.

	Membranes			
	PolyAl TypM1	PolyAn	Pervap 2255-30	Pervap 2256
A_{min},A(m^2)	1410, 1760	3080, 3850	2510, 3140	1430, 1790
Q_R (kW)	4070	3250	2420	3530
Theoretical and actual number of trays of C_1	18, 28	18, 28	18, 28	16, 25
Diameter of C_1 (m)	2.34	2.44	2.80	2.09
Q_{C1} (kW)	6030	6590	8760	4760
A_{C1} (m^2)	546	596	793	431
Q_{B1} (kW)	5750	6280	8350	4550
A_{B1} (m^2)	86	94	125	68
Theoretical and actual number of trays of C_2	22, 34	27, 42	24, 37	20, 31
Diameter of C_2 (m)	2.96	2.80	2.56	2.80
Q_{C2} (kW)	13,660	12,270	10,260	12,220
A_{C2} (m^2)	1237	1110	928	1106
Q_{B2} (kW)	14,810	13,310	11,120	13,240
A_{B2} (m^2)	253	227	190	226
Pervaporation unit investment (10^6 U$S/year)	2.10	4.60	3.75	2.14
Distillation columns investment (10^6 U$S/year)	1.56	1.64	1.60	1.35
Pervaporation unit utilities (10^6 U$S/year)	3.66	6.23	5.35	3.49
Distillation columns utilities (10^6 U$S/year)	5.23	4.98	4.97	4.52
General cost (10^6 U$S/year)	2.11	3.54	3.05	2.02
Overall cost of separation (10^6 U$S/year)	13.4	17.1	15.1	12.1

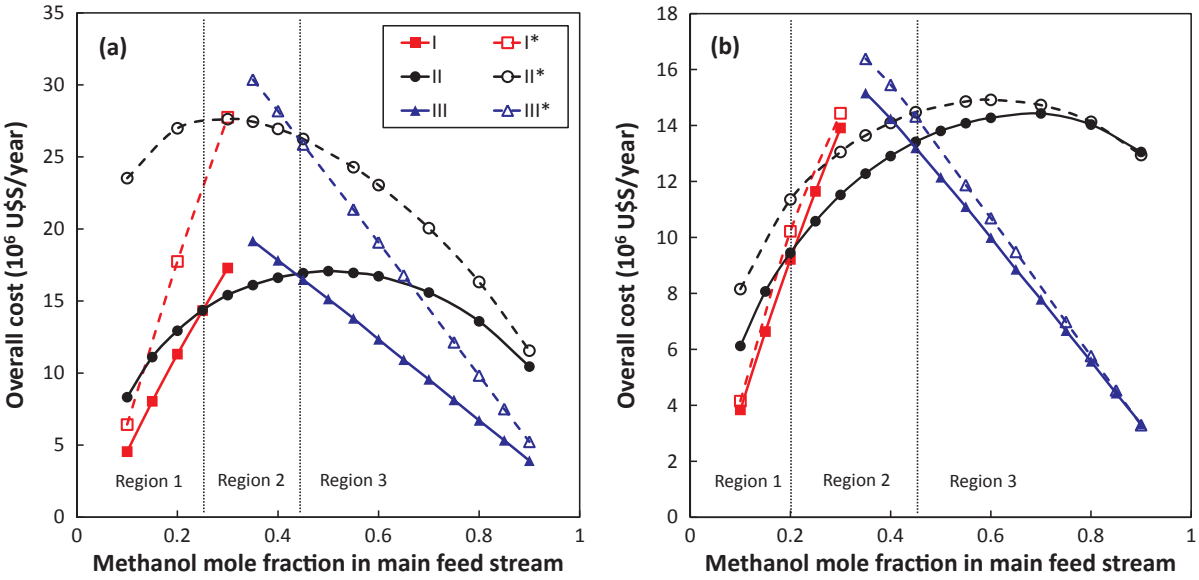

Fig. 9. Overall cost versus main feed composition for several hybrid process configurations with a (a) Pervap 2255-30 or a (b) Pervap 2256 membrane. (T_{op} = 348.15 K). The overall cost at each point corresponds to the optimal design.

feed is nearer to that of one of the product specifications (either 0.056 or 0.99 mol/mol) because in these cases the separation effort is lower.

For the design with the Pervap 2255-30 membrane (Fig. 9a), the overall costs of separation for the configurations I∗, II∗, III∗ are much higher than those for the configurations I, II and III, respectively. While optimal values for the retentate composition are relatively far from the specification of the methyl acetate rich product (0.056 mol/mol in methanol) in the case of configurations with the Pervap 2255-30 membrane, optimal retentate compositions for configurations with the Pervap 2256 membrane are much closer to the mentioned specification. As a consequence, the difference between of the overall cost corresponding to each pair of configurations I-I∗, II-II∗ and III and III∗ is much lower for the designs corresponding to the Pervap 2256 membrane (Fig. 9b).

Optimal process configuration strongly depends on feed composition (Fig. 9a and b). For both Pervap membranes, configuration I presents the lowest overall cost for feed compositions belonging Region 1. In this region, investment and operating costs corresponding to distillation column C1 govern the overall cost of separation. For feed compositions in Region 2, configuration II is the most suitable. Here, the pervaporation process has a major contribution in the overall separation cost. Finally, configuration III is the preferred one in the wide compositions interval of Region 3.

For all studied membranes, Fig. 10a and b show the overall cost of the separation as function of the feed composition for two operating temperatures in the pervaporation unit; i.e. 318.15 and 348.15 K, respectively. Each point in Fig. 10a and b corresponds to the optimal process configuration.

In both figures, the overall cost curves corresponding to each membrane are clearly separated among them. For these curves, a high difference in cost occurs at feed compositions values in the interval [0.35, 0.45 mol/mol]. In this interval, membranes can be easily ranked

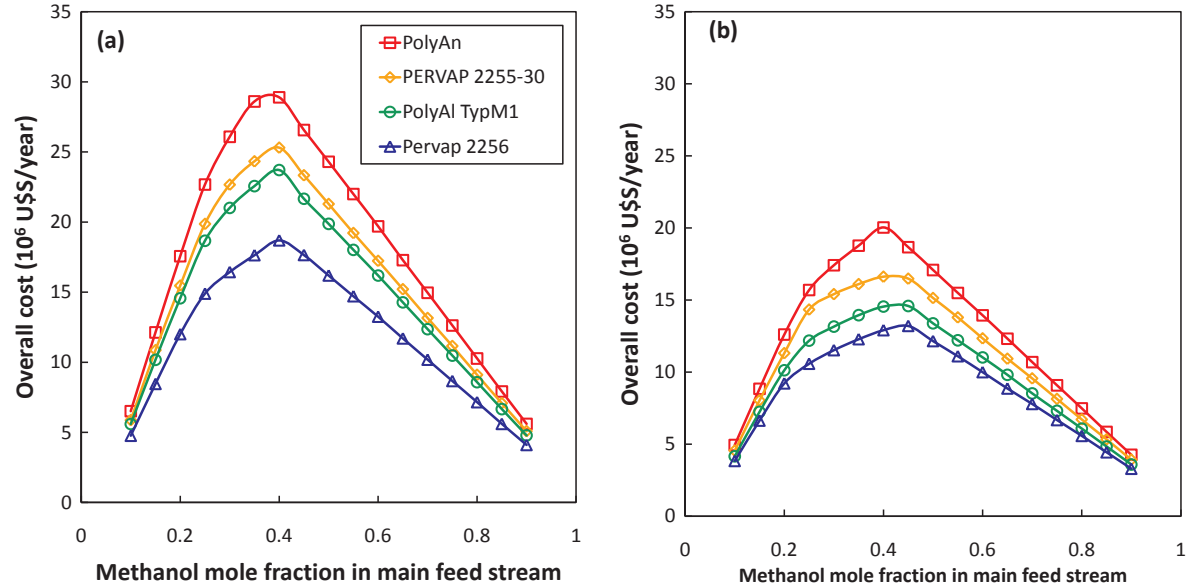

Fig. 10. Overall cost versus main feed composition for operating temperatures in the pervaporation unit of (a) 318.15 and (b) 348.15 K. The overall cost at each point corresponds to the optimal hybrid process configuration.

according to their respective overall cost of separation. In accordance with this criterion, the design corresponding to the Pervap 2256 membrane is the less costly followed by the designs corresponding to the PolyAl TypM1, Pervap 2255-30, and PolyAn membranes.

From the comparison between Fig. 10a and b, it is observed that for all membranes the lowest values of the overall separation cost are achieved at 348.15 K. For all cases shown in Fig. 10b, the decrease in the investment cost of the pervaporation unit triggered by the increase in the operating temperature is much higher than the increment of the operating cost involved in the retentate heating.

As mentioned, the PolyAl TypM1 and PolyAn membranes can work at temperatures above 348.15 K. For this reason, the designs corresponding to these membranes are evaluated at 363.15 K and compared with the designs of the Pervap membranes working at 348.15 K. Results are presented in Fig. 11.

From Fig. 11, it is noted that the designs with the PolyAl TypM1 and Pervap 2256 membranes are the less costly ones. For the remaining two membranes, the resulting overall costs are up to 30% higher than those corresponding to the PolyAl TypM1 and Pervap 2256 membranes.

3.3.1. Sensitivity analysis

Results of sensitivity analysis are shown in Fig. 12a and b for a feed composition of 0.4 mol/mol. For each membrane, the overall costs corresponding to the optimal configuration II were recalculated by varying the cost factors related to the investment cost of the pervaporation unit (Fig. 12a) and the purchase cost of the membrane module (Fig. 12b).

Overall, the total costs of separation for the designs with the PolyAn and Pervap 2255-30 membranes are more sensitive to changes in the sensitivity variables than those corresponding to PolyAl TypM1 and Pervap 2256 membranes. Required membrane areas for the PolyAl TypM1 and Pervap 2256 membranes are much lower than the area requirement for the PolyAn and Pervap 2255-30 membranes. Thus, their respective total cost is less sensitive to the investment cost of the pervaporation unit.

Results showed that the even considering a ± 25% in the variation of the factor for the investment cost estimation of the pervaporation unit, the Pervap 2256 and PolyAl TypM1 membranes remain as the best candidates. In a similar way, Fig.12b shows that the Pervap 2256 and PolyAl TypM1 membranes are promissory candidates in the entire range of variation of the purchase cost of the membrane module [± 15, ± 75%].

From the comparison above, it is concluded that the calculation of the investment cost of the pervaporation unit from a cost factor per membrane area implies a high uncertainty in the contribution of the vacuum condensing system into the overall cost.

Therefore, in order to make more precise cost estimations, the modeling of the vacuum condensing system is necessary. Moreover, the permeate pressure can then be considered as an optimization variable to capture the trade-off between the operating cost of vacuum condensing system and the investment cost of the membrane module.

3.3.2. Design of vacuum condensing system

For the separation of a mixture of composition 0.85 mol/mol in methanol, Table 6 presents optimal values for retentate and distillates compositions, equipment sizes and energy duties corresponding to process configuration II. In this case, a detailed modeling of the vacuum condensing system is taken into account in the process design. An operating temperature of 348.15 K and permeate pressures of either 10 or 100 mbar are adopted for the pervaporation unit with the Pervap 2256 membrane. In Table 6, values for optimization variables are shown in bold.

The membrane area requirement for an operating permeate pressure of 100 mbar is 50% higher than that corresponding to 10 mbar. As a consequence, the investment cost of the membrane module is higher at 100 mbar. On the other hand, for an operating permeate pressure of 100 mbar, the overall energy demand of both columns is slightly slower than that corresponding to 10 mbar.

Regarding to the vacuum condensing system, for an operating permeate pressure of 10 mbar, the temperature required for condensing the permeate stream is about 237 K while a condensation temperature of 272 K is required at 100 mbar. This mild operating condition gives rise to a most economic design of the refrigeration system. In fact, the refrigeration system corresponding at 100 mbar requires about 45% less energy than that at 10 mbar. Moreover, given that at 100 mbar the refrigeration system does not require multistep configuration, the investment cost is also cheaper at this condition.

Summarizing and taking into account both investment and operating cost, the overall separation cost (last row in Table 6) is 14% lower for a permeate pressure of 100 than that of 10 mbar. Considering the permeate pressure as an optimization variable in the interval [10, 100 mbar], the optimum value for this variable approached its upper bound, which in turn was the maximum permeate pressure considered at experiments done with the Pervap 2256 membrane.

Conditions of feed and product streams for this case example are very similar with those reported design by retrofitting in Genduso et al. [3]. Both lower values for the membrane area requirement and the energy consumption are obtained when the optimization based design proposed in this manuscript is adopted. This approach overcomes limitations inherent to optimal designs found from the retrofitting of existing processes.

4. Conclusions

In this manuscript, the performance of four methanol-selective membranes (Pervap 2255-30, Pervap 2256, PolyAn and PolyAl TypM1) for the separation of the methanol-methyl acetate mixture was assessed.

For the commercial Pervap 2256 membrane, pervaporation experiments were carried out in order to characterize its flux and selectivity. Results showed that this membrane is capable of breaking the methanol-methyl acetate azeotrope. In particular, for feed compositions around that the azeotrope, a maximum overall flux about 18 kg/(m^2 h) with a separation factor about 3 was obtained at 348.15 K and 5mbar.

It is noteworthy that, except for the PolyAl TypM1 membrane which shows a performance well above than those for the Pervap 2255-30, Pervap 2256 and PolyAn membranes in the whole range of retentate

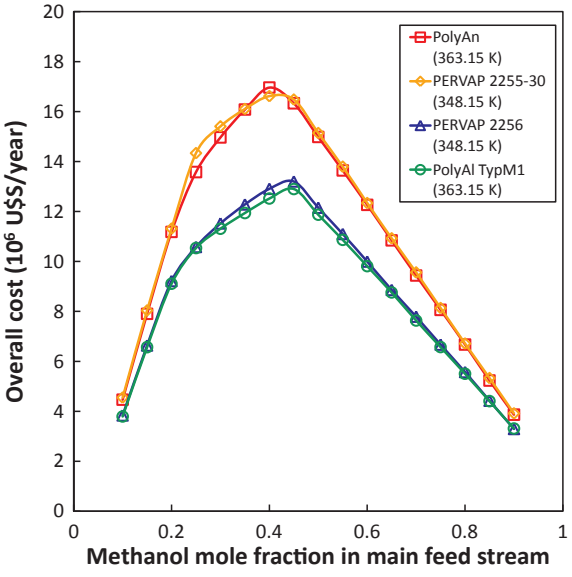

Fig. 11. Overall cost versus main feed composition. Operating temperature in the pervaporation unit of 348.15 K for the Pervap membranes and of 363.15 K for the PolyAn and PolyAl TypM1 membranes. The overall cost at each point of composition corresponds to the optimal hybrid process configuration.

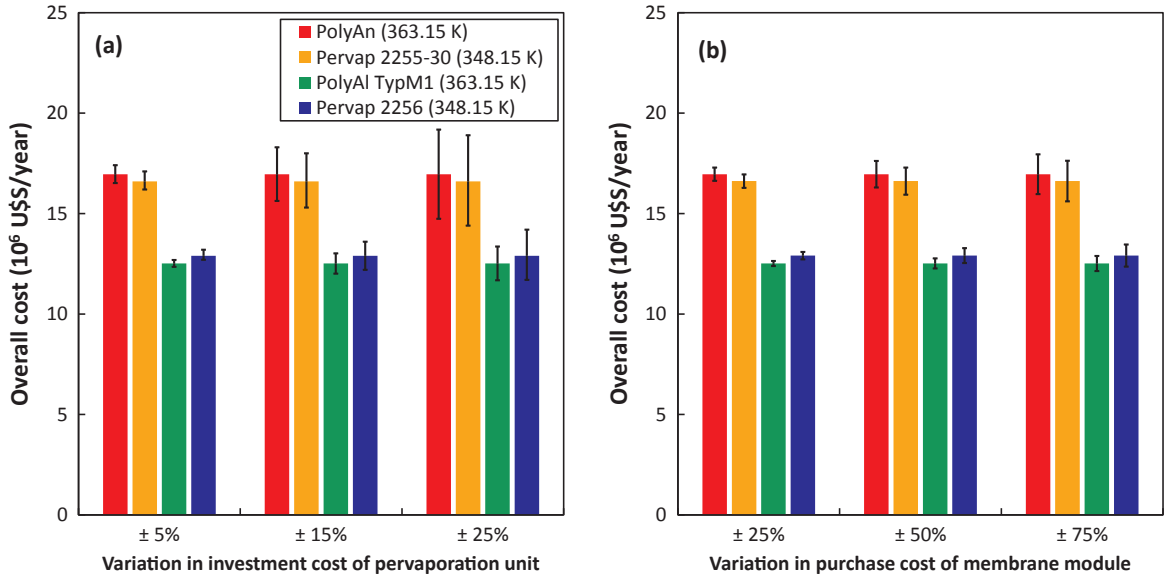

Fig. 12. Sensitivity analysis of the total cost varying (a) the investment cost of the pervaporation unit and (b) the purchase cost of the membrane module. (x_0 = 0.4 mol/mol).

Table 6
Equipment sizes, energy requirements and total cost of the process configuration II with the Pervap 2256 membrane. A detailed design of the vacuum condensing system is included. (x_0 = 0.85 mol/mol, T_{op} = 348.15 K). Additional specifications for the refrigeration system are presented in Table SM19 (Supplementary material).

	Permeate pressure p (mbar)	
	10	**100**
x_R,y_P(mol/mol)	**0.142**, 0.543	**0.123**, 0.537
x_{D1} **(mol/mol)**	**0.300**	**0.296**
x_{D2} **(mol/mol)**	**0.346**	**0.346**
A_{min},A(m^2)	412, 515	617, 771
Q_R (kW)	981	1020
A_R (m^2)	30	30
Theoretical and actual number of trays of C_1	14, 22	13, 20
Diameter of C_1 (m)	1.06	0.95
Q_{C1} (kW)	−1210	−954
A_{C1} (m^2)	110	86
Q_{B1} (kW)	1160	913
A_{B1} (m^2)	18	14
Theoretical and actual number of trays of C_2	22, 34	22, 34
Diameter of C_2 (m)	1.79	1.80
Q_{C2} (kW)	−4780	−4840
A_{C2} (m^2)	432	438
Q_{B2} (kW)	5180	5250
A_{B2} (m^2)	89	90
T_{cond}^{end} (K)	237	272
W_P(kW)	2.2	2.2
W_{VP}(kW)	14	2
Q_P (kW)	1400	1320
A_{VC} (m^2)	626	602
W_{Comp} 1,2 (kW)	310, 526	460
A_{RC} (m2)	409	327
Membrane module investment (10^6 U$S/year)	0.13	0.17
Vacuum condensing system investment (10^6 U$S/year)	0.55	0.38
Distillation columns investment (10^6 U$S/year)	0.77	0.75
Membrane module utilities (10^6 U$S/year)	0.24	0.26
Vacuum condensing system utilities (10^6 U$S/year)	1.01	0.57
Distillation columns utilities (10^6 U$S/year)	1.61	1.56
General cost (10^6 U$S/year)	0.87	0.79
Overall cost of separation (10^6 U$S/year)	5.18	4.48

compositions studied (Fig. 8), the PSI analysis is not appropriate to obtain a ranking among the membranes.

Thus, the membrane performance was assessed based on the conceptual design of different configurations of the pervaporation-distillation hybrid process. Considering the minimization of the overall cost of separation, the optimization of the design corresponding to each membrane was achieved by considering the compositions of the retentate and distillate streams as optimization variables. Following this methodology, the membranes were successfully ranked in accordance with their respective overall separation cost.

The best-ranked membranes, which have similar overall costs, were the PolyAl TypM1 and the Pervap 2256 membranes. The present methodology proved to be more adequate and consistent for performance assessment than judging it using the PSI.

Furthermore, a sensitivity analysis was performed to consider the variation in the purchase cost among the membranes. Results showed that the membrane ranking is still valid even considering ± 75% variations in the membrane purchase cost. In addition, it was concluded that the calculation of the investment cost of the pervaporation unit from a cost factor per membrane area implies a high uncertainty in the contribution of the vacuum condensing system into the overall cost. Then a more detailed modeling of the vacuum condensing system is paramount when more precise cost estimations are desired.

From the detailed design of the vacuum condensing system, it was noted that including the permeate pressure as an optimization variable allowed to properly capture trade-offs between the investment cost of the membrane module and the investment and operating cost of the vacuum condensing system. For the Pervap 2256 membrane, the optimal value of the permeate pressure was 100 mbar with a condensation temperature about 272 K.

Acknowledgements

The authors gratefully acknowledge CONICET (Argentina) for the financial support through project PIP 688.

Appendix A. Supplementary material

Supplementary data associated with this article can be found, in the online version, at http://dx.doi.org/10.1016/j.seppur.2017.08.027.

References

[1] T. Melin, R. Rautenbach, Membranverfahren: Grundlagen der Modul-und Anlagenauslegung, Springer-Verlag, 2007.
[2] B. Van der Bruggen, P. Luis, Pervaporation, in: Steve Tarleton (Ed.), Prog. Filtr.

Sep., Academic Press, Oxford, 2015: pp. 101–154. 10.1016/B978-0-12-384746-1.00004-5.
[3] G. Genduso, A. Amelio, E. Colombini, P. Luis, J. Degrève, B. Van der Bruggen, Retrofitting of extractive distillation columns with high flux, low separation factor membranes: A way to reduce the energy demand? Chem. Eng. Res. Des. 109 (2016) 127–140, http://dx.doi.org/10.1016/j.cherd.2016.01.013.
[4] J. Bausa, W. Marquardt, Shortcut design methods for hybrid membrane/distillation processes for the separation of nonideal multicomponent mixtures, Ind. Eng. Chem. Res. 39 (2000) 1658–1672, http://dx.doi.org/10.1021/ie990703t.
[5] W. Stephan, R.D. Noble, C.A. Koval, Design methodology for a membrane/distillation column hybrid process, J. Memb. Sci. 99 (1995) 259–272, http://dx.doi.org/10.1016/0376-7388(94)00255-W.
[6] V. Van Hoof, L. Van den Abeele, A. Buekenhoudt, C. Dotremont, R. Leysen, Economic comparison between azeotropic distillation and different hybrid systems combining distillation with pervaporation for the dehydration of isopropanol, Sep. Purif. Technol. 37 (2004) 33–49, http://dx.doi.org/10.1016/j.seppur.2003.08.003.
[7] P. Kreis, A. Górak, Process analysis of hybrid separation processes: combination of distillation and pervaporation, Chem. Eng. Res. Des. 84 (2006) 595–600, http://dx.doi.org/10.1205/cherd.05211.
[8] F. Lipnizki, R.W. Field, P.-K. Ten, Pervaporation-based hybrid process: a review of process design, applications and economics, J. Memb. Sci. 153 (1999) 183–210, http://dx.doi.org/10.1016/S0376-7388(98)00253-1.
[9] S. Steinigeweg, J. Gmehling, Transesterification processes by combination of reactive distillation and pervaporation, Chem. Eng. Process. Process Intensif. 43 (2004) 447–456, http://dx.doi.org/10.1016/S0255-2701(03)00129-6.
[10] Y. Fuchigami, Hydrolysis of methyl acetate in distillation column packed with reactive packing of ion exchange resin, J. Chem. Eng. Japan. 23 (1990) 354–359, http://dx.doi.org/10.1252/jcej.23.354.
[11] L. Jimenez, A. Garvin, J. Costa-Lopez, The production of butyl acetate and methanol via reactive and extractive distillation. II. Process modeling, dynamic simulation and control strategy, Ind. Eng. Chem. Res. 41 (2002) 6735–6744, http://dx.doi.org/10.1021/ie0107643.
[12] W.L. Luyben, Design and control of the butyl acetate process, Ind. Eng. Chem. Res. 50 (2011) 1247–1263, http://dx.doi.org/10.1021/ie100103r.
[13] P. Langston, N. Hilal, S. Shingfield, S. Webb, Simulation and optimisation of extractive distillation with water as solvent, Chem. Eng. Process. Process Intensif. 44 (2005) 345–351, http://dx.doi.org/10.1016/j.cep.2004.05.008.
[14] Z. Zhang, Q. Zhang, G. Li, M. Liu, J. Gao, Design and control of methyl acetate-methanol separation via heat-integrated pressure-swing distillation, Chinese J. Chem. Eng. 24 (2016) 1584–1599, http://dx.doi.org/10.1016/j.cjche.2016.06.013.
[15] S. Sain, S. Dincer, Ö. Savaşçyı, Pervaporation of methanol–methyl acetate binary mixtures, Chem. Eng. Process. Process Intensif. 37 (1998) 203–206, http://dx.doi.org/10.1016/S0255-2701(97)00058-5.
[16] D. Gorri, R. Ibáñez, I. Ortiz, Comparative study of the separation of methanol–methyl acetate mixtures by pervaporation and vapor permeation using a commercial membrane, J. Memb. Sci. 280 (2006) 582–593, http://dx.doi.org/10.1016/j.memsci.2006.02.016.
[17] T. Brinkmann, H. Pingel, T. Wolff, M. Döker, E. Bozek-Winkler, J. Gmehling, Verhalten Verschiedener Membranmaterialien für die Aufbereitung Organischer Produktströme aus Reaktivrektifikationskolonnen, Chemie Ing. Tech. 80 (2008) 157–164, http://dx.doi.org/10.1002/cite.200700170.
[18] J. Gmehling, Development, validation and evaluation of reactive distillation processes coupled to different separation stages (pervaporation, extractive distillation and azeotropic distillation), Oldenburg, Germany, 2008 http://www.tchemie.uni-oldenburg.de/download/Berichte/Abschlussbericht_AIF14515.pdf.
[19] H. Matuschewski, U. Schedler, MSE - modified membranes in organophilic pervaporation for aromatics/aliphatics separation, Desalination 224 (2008) 124–131, http://dx.doi.org/10.1016/j.desal.2007.04.083.
[20] A. Fahmy, D. Mewes, K. Ebert, Design methodology for the optimization of membrane separation properties for hybrid vapor permeation-distillation processes, Sep. Sci. Technol. 36 (2001) 3287–3304, http://dx.doi.org/10.1081/SS-100107903.
[21] M.A. Sosa, D.A. Figueroa Paredes, J.C. Basílico, B. Van der Bruggen, J. Espinosa, Screening of pervaporation membranes with the aid of conceptual models: an application to bioethanol production, Sep. Purif. Technol. 146 (2015) 326–341, http://dx.doi.org/10.1016/j.seppur.2015.04.001.
[22] W. Marquardt, S. Kossack, K. Kraemer, A framework for the systematic design of hybrid separation processes, Chinese J. Chem. Eng. 16 (2008) 333–342, http://dx.doi.org/10.1016/S1004-9541(08)60084-1.
[23] J.A. Caballero, I.E. Grossmann, M. Keyvani, E.S. Lenz, Design of hybrid distillation-vapor membrane separation systems, Ind. Eng. Chem. Res. 48 (2009) 9151–9162, http://dx.doi.org/10.1021/ie900499y.
[24] K. Koch, D. Sudhoff, S. Kreiß, A. Górak, P. Kreis, Optimisation-based design method for membrane-assisted separation processes, Chem. Eng. Process. Process Intensif. 67 (2013) 2–15, http://dx.doi.org/10.1016/j.cep.2012.09.013.
[25] M. Skiborowski, J. Wessel, W. Marquardt, Efficient optimization-based design of membrane-assisted distillation processes, Ind. Eng. Chem. Res. 53 (2014) 15698–15717, http://dx.doi.org/10.1021/ie502482b.
[26] K. Koch, A. Górak, Pervaporation of binary and ternary mixtures of acetone, isopropyl alcohol and water using polymeric membranes: experimental characterisation and modelling, Chem. Eng. Sci. 115 (2014) 95–114, http://dx.doi.org/10.1016/j.ces.2014.02.009.
[27] MathWorks, MATLAB User's Guide, (1993).
[28] B. Efron, R.J. Tibshirani, An introduction to the bootstrap, CRC Press, Boca Raton FL, 1993.
[29] M. Luna, E. Martínez, A Bayesian approach to run-to-run optimization of animal cell bioreactors using probabilistic tendency models, Ind. Eng. Chem. Res. 53 (2014) 17252–17266, http://dx.doi.org/10.1021/ie500453e.
[30] G. Genduso, P. Luis, B. Van der Bruggen, Overcoming any configuration limitation: an alternative operating mode for pervaporation and vapour permeation, J. Chem. Technol. Biotechnol. 91 (2016) 948–957, http://dx.doi.org/10.1002/jctb.4661.
[31] T. Pöpken, L. Götze, J. Gmehling, Reaction kinetics and chemical equilibrium of homogeneously and heterogeneously catalyzed acetic acid esterification with methanol and methyl acetate hydrolysis, Ind. Eng. Chem. Res. 39 (2000) 2601–2611, http://dx.doi.org/10.1021/ie000063q.
[32] Aspen Distil and Aspen Hysys User Manual Version 8, (2014).
[33] M.F. Doherty, M.F. Malone, Conceptual design of distillation systems, McGraw-Hill Science/Engineering/Math, New York, 2001.
[34] W.L. Mccabe, E.W. Thiele, Graphical design of fractionating columns, Ind. Eng. Chem. 17 (1925) 605–611, http://dx.doi.org/10.1021/ie50186a023.
[35] J.R. Fair, How to predict sieve tray entrainment and flooding, Petro/Chem Eng. 33 (1961) 45–62.
[36] S. Le Digabel, NOMAD: nonlinear optimization with the MADS Algorithm, Optimization. 37 (2011) 1–15, http://dx.doi.org/10.1145/1916461.1916468.
[37] J. Currie, D.I. Wilson, OPTI, lowering the barrier between open source optimizers and the industrial MATLAB user, Found. Comput, Process Oper, 2012.